Electronic Supplementary Material (ESI) for Journal of Materials Chemistry C.

Supporting Information

Lignin-derived Porous Graphene for Wearable and Ultrasensitive Strain Sensors

Shuhong Yang [a], Yun Ling [a], Qian Wu [b], Hanwen Zhang [a], Zheng Yan [a,b], Guoliang Huang [b], Jian Lin [b], Caixia Wan [a, *]

[a] Department of Biomedical, Biological, and Chemical Engineering, University of Missouri, Columbia 65211, USA

[b] Department of Mechanical and Aerospace Engineering, University of Missouri, Columbia 65211, USA

[*]Corresponding author: Phone: +1 573 884 7882; Fax: +1 573 884 5650; E-mail: wanca@missouri.edu

Number of Pages: 12

Number of Tables: 2

Number of Figures: 7

Calculation of gauge factor and hysteresis

Gauge factor (GF) was calculated by Equation S1:

$$GF = \frac{(R-R_0)/R_0}{\varepsilon} \quad \text{(S1)}$$

Where R is resistance, R_0 is original resistance, ε is strain calculated based on relative length change (ΔL) divided by original length (L).

Hysteresis was calculated by Equation S2:

$$h\% = \left|\frac{R_s-R_r}{R_{max}}\right| \times 100\% \quad \text{(S2)}$$

Where R_s, R_r, and R_{max} are the stretching, releasing, and maximum values of resistance at a given strain, respectively.

Table S1. Sheet resistance of LIG from various precursors

Precursor for LIG	Rs (Ω/square) *	Reference
Lignin	4.5	This work
Wood	~10	[1]
Cellulose paper	32	[2]
Polyimide	~17	[3]
Polyetherimide	~15	[4]
Phenolic resin	~40	[5]

* Lowest sheet resistance (Rs) obtained for comparison.

Table S2. Performance comparisons of state-of-art strain sensors

Sensing materials	Working Range	Gauge factor	Limits of strain detection	Hysteresis	Tested Stability	Reference
Lignin-derived LIG/ Dragon Skin™	9%-14%	960	0.1%	7% at <9% strain	10,000	This work
	4%~9%	166				
	0.1%~4%	100				
Paper-derived LIG	0.2%~1%	41.9	~0.2%	Not shown	~2,500	[2]
LIG derived from lignin-PDMS	65%	20	Not shown	3% at <60% strain	5,000	[6]
PI-derived LIG	<1.5%	26	Not shown	Not shown	20,000	[7]
PI-derived LIG/PDMS composite	<30%	160	Not shown	Not shown	200	[8]
PI-LIG/Kapton tape	<3.3%	0.47	Not shown	Not shown	1,300	[9]
Graphene oxide/PDMS	<2%	34.3	Not shown	Not shown	Not shown	[10]
	2%~5%	99.9				
	5%~7.5%	402.3				
CVD-grown graphene/PDMS	0.3%~4.5%	151	0.3%	Not shown	Not shown	[11]
Graphene woven fabrics/PDMS	<2%	35	Not shown	Not shown	100	[12]
	2%~6%	1000				
CNT-based conductive paper	0.1%~0.7%	2.6-7.5	0.1%	Not shown	1,000	[13]
CVD-based carbon nanotube/ Ecoflex	0.1%~80%	256	0.1%	~50%* at <140% strain	1,000	[14]
	80%~145%	3250				
CNT/PDMS	<40%	0.8	Not shown	~72%* at <200% strain	10,000	[15]
	40%~280%	0.06				
Silver nano wire composites/ PDMS	<70%	14	Not shown	25%~66%*	1,000	[16]
Nanowire/PDMS	<1.08%	35.8	Not shown	<8.1%	~1,200	[17]

* Values estimated from publications.

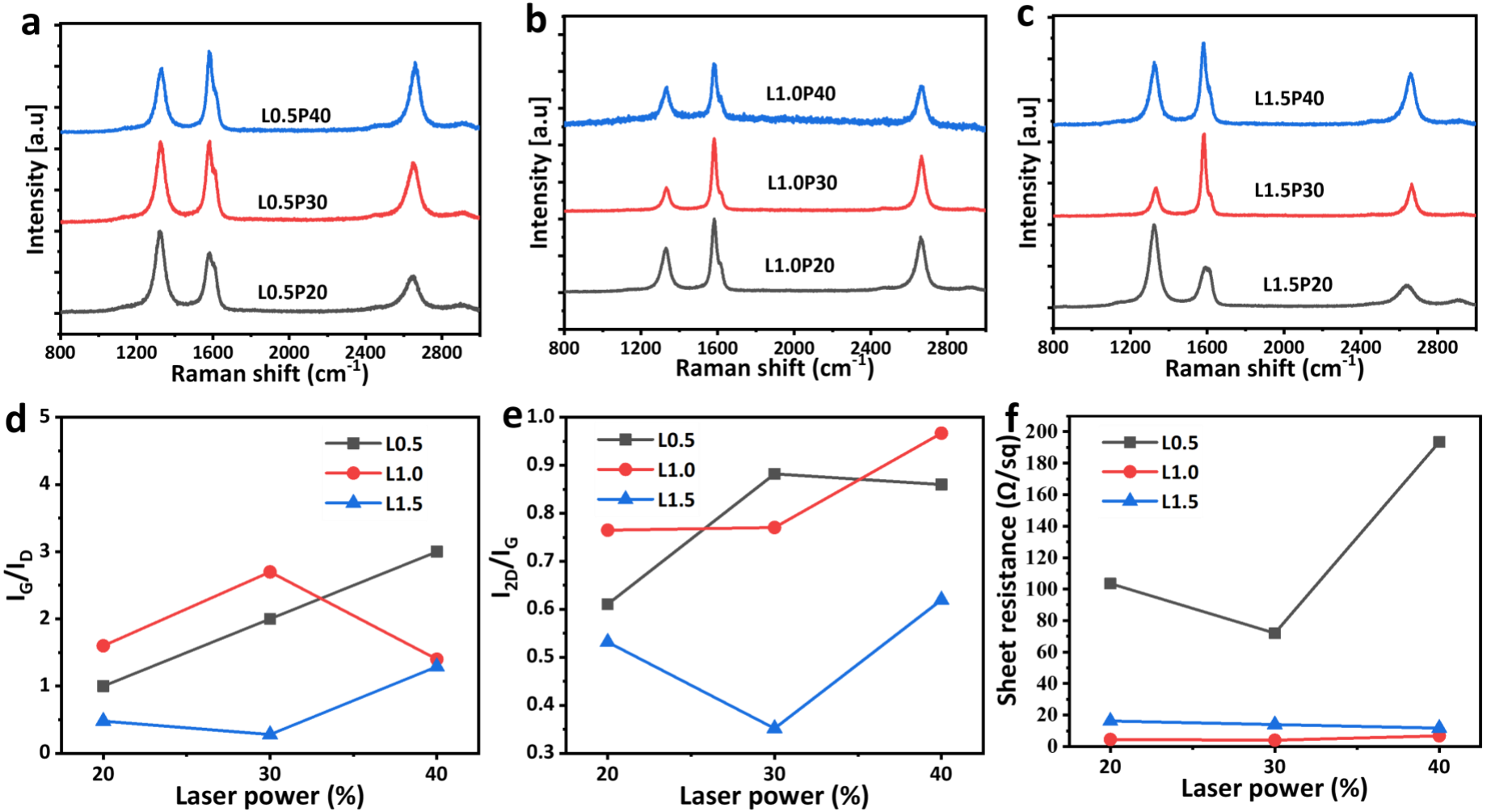

Fig. S1. Characteristics of LIG. (a-c) Raman spectra. (d, e) I_G/I_D and I_{2D}/I_G, respectively. (f) Sheet resistance. L0.5, L1.0, and L1.5 stand for respective lignin loadings in the three films. P20, P30, and P40 stand for 20%, 30%, and 40% power level, respectively.

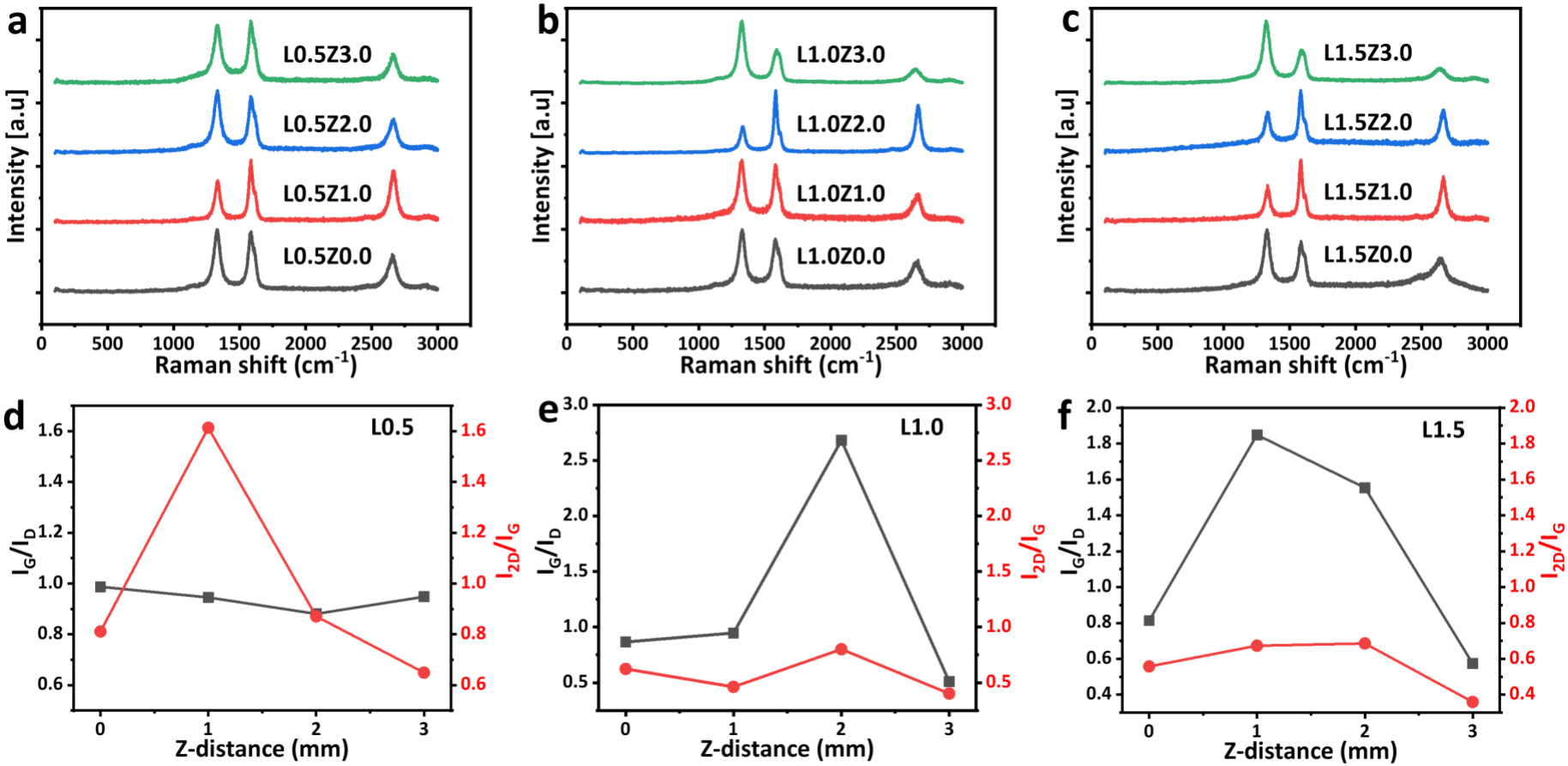

Fig. S2. Characteristics of LIG. (a-c) Raman spectra. (d-f) I_G/I_D and I_{2D}/I_G. L0.5, L1.0, and L1.5 stand for respective lignin loadings in the three films. Z0.0, Z1.0, Z2.0 and Z3.0 stand for 0.0-, 1.0-, 2.0-, and 3.0-mm z-axis defocus distance, respectively. All the LIG samples were obtained at 30% laser power.

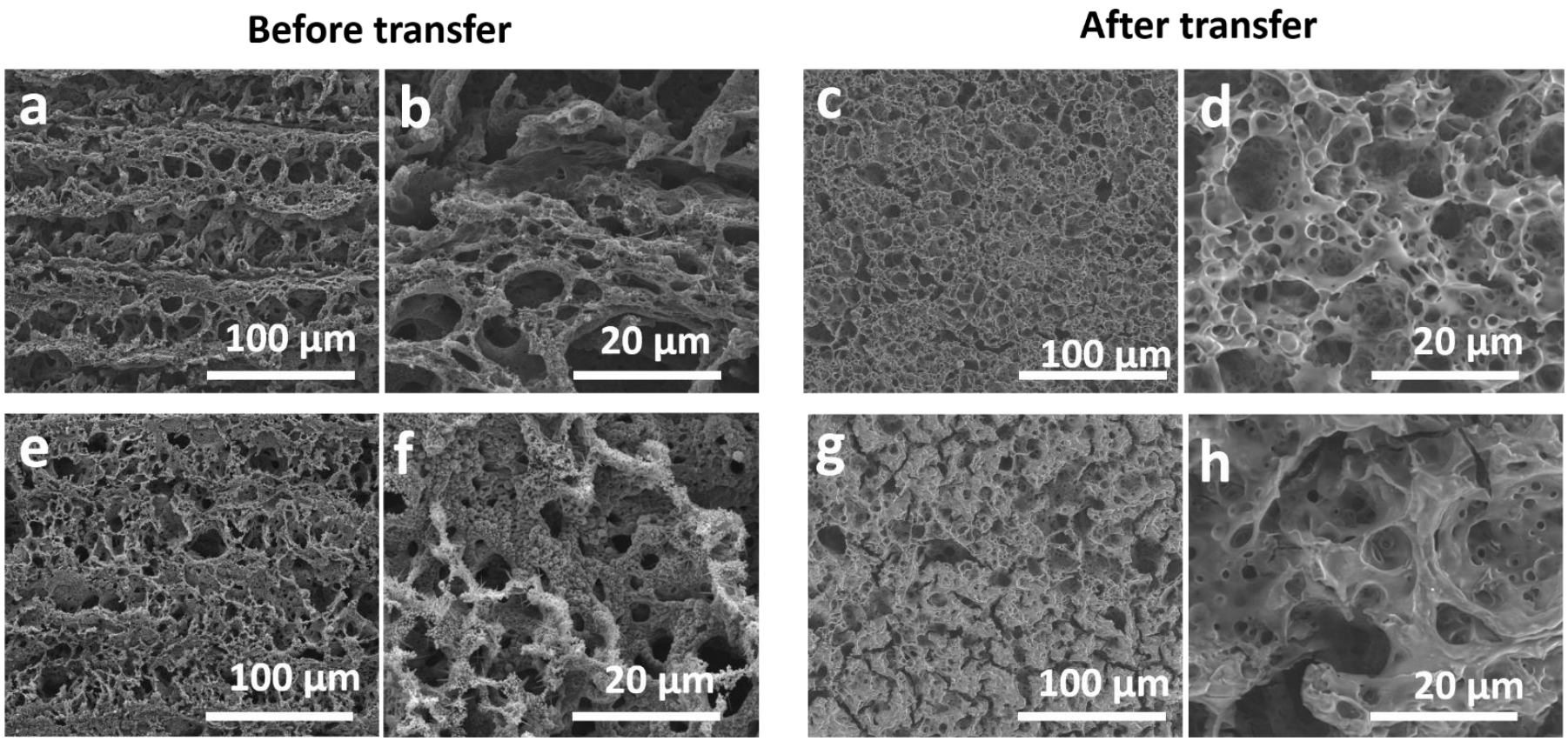

Fig. S3. SEM images of LIG samples. (a-b) L1.0P20 before transfer; (c-d) L1.0P20 after transfer. (e-f) L1.0P40 before transfer; (g-h) L1.0P40 after transfer. Scale bar: 100 µm (a, c, e, g), and 20 µm (b, d, f, h).

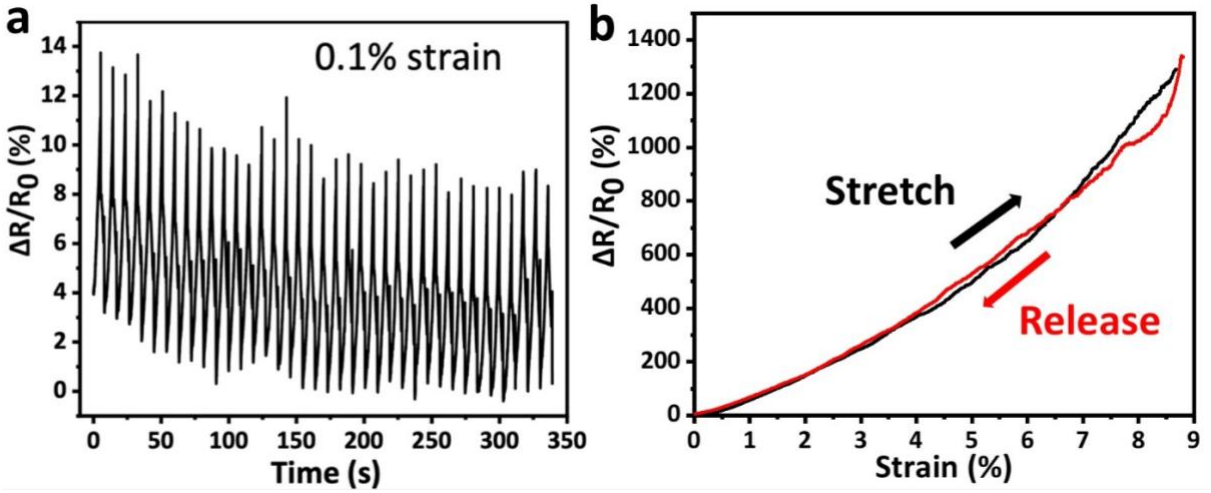

Fig. S4. (a) Strain sensor working at 0.1% strain for about 40 stretch-release cycles. (b) $\Delta R/R_0$ when stretched (black line) and released (red line) at 9% strain.

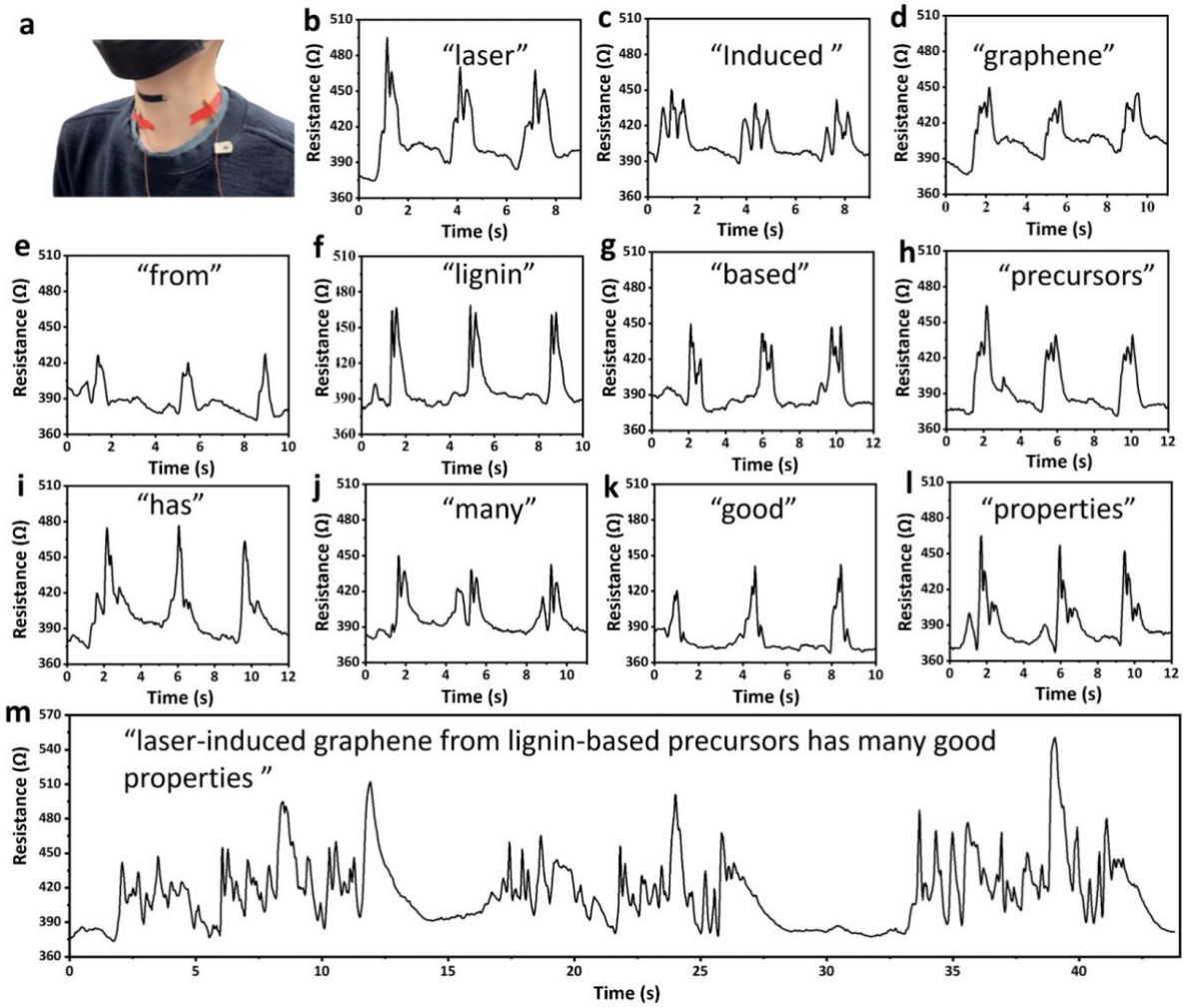

Fig. S5. Strain sensor working as a speaking detector. (a) Photo of attaching the sensor to one's throat. Signal patterns when one speaks (b-i) individual words and (m) a whole sentence three times.

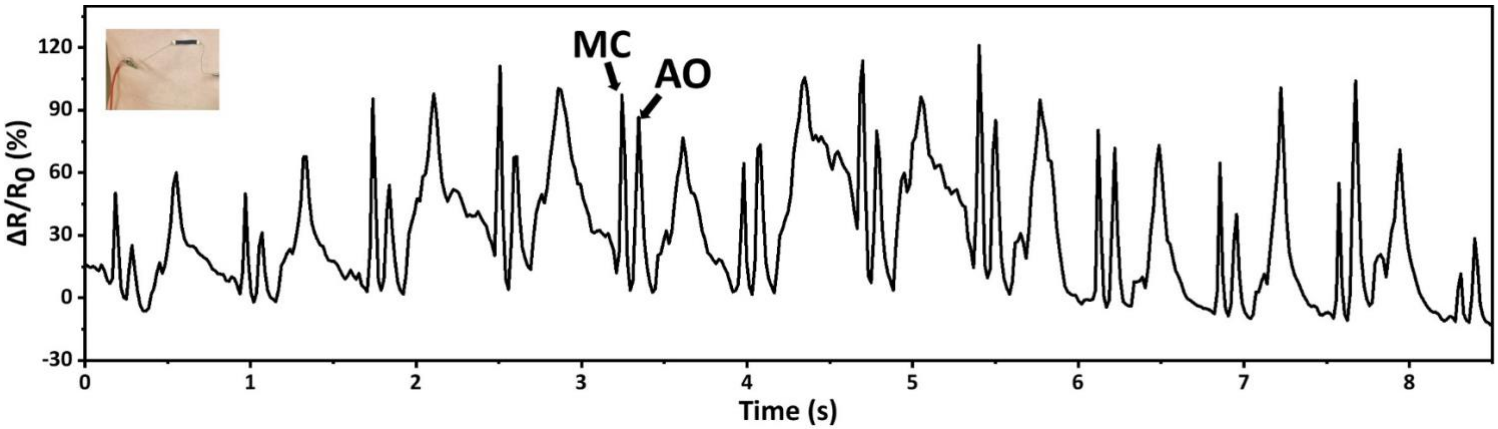

Fig. S6. $\Delta R/R_0$ of seismocardiography detected at lower chest (shown in the photo) when one's breath is being held.

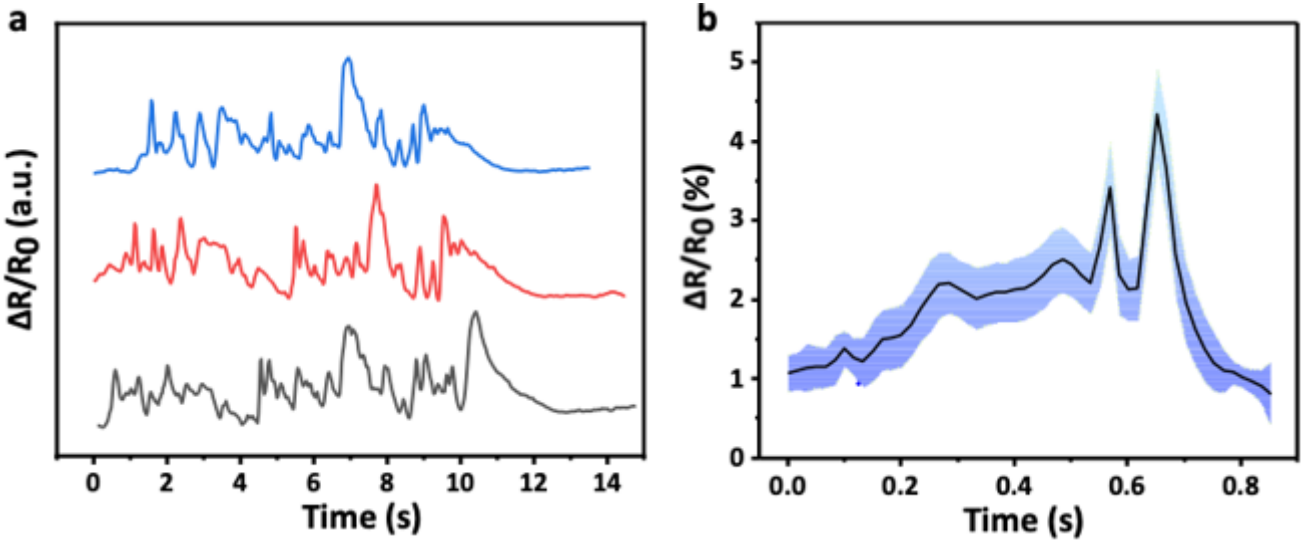

Fig. S7. Signal analysis of speaking and seismocardiography. (a) Comparison of speaking signals presented in Fig.S5m in parallel. (b) Mean and standard deviation of seismocardiographic signals.

References

1. R. Ye, Y. Chyan, J. Zhang, Y. Li, X. Han, C. Kittrell and J.M. Tour, Laser-induced graphene formation on wood, *Adv. Mater.*, 2017, **29**(37), 170221.
2. B. Kulyk, B.F.R. Silva, A.F. Carvalho, S. Silvestre, A.J.S. Fernandes, R. Martins, E. Fortunato and F.M. Costa, Laser-induced graphene from paper for mechanical sensing, *ACS Appl. Mater. Interfaces*, 2021, **13**(8), 10210-10221.
3. J. Lin, Z. Peng, Y. Liu, F. Ruiz-Zepeda, R. Ye, E.L. Samuel, M.J. Yacaman, B.I. Yakobson and J.M. Tour, Laser-induced porous graphene films from commercial polymers, *Nat. Commun.*, 2014, **5**, 5714.
4. A. Al-Rahayfeh and M. Faezipour, Eye tracking and head movement detection: a state-of-art survey, *IEEE J. Transl. Eng. Health Med.*, 2013, **1**, 2100212.
5. Z.C. Zhang, M.M. Song, J.X. Hao, K.B. Wu, C.Y. Li and C.G. Hu, Visible light laser-induced graphene from phenolic resin: a new approach for directly writing graphene-based electrochemical devices on various substrates, *Carbon*, 2018, **127**, 287-296.
6. C.W. Lee, S.Y. Jeong, Y.W. Kwon, J.U. Lee, S.C. Cho and B.S. Shin, Fabrication of laser-induced graphene-based multifunctional sensing platform for sweat ion and human motion monitoring, *Sens. Actuator A Phys.*, 2022, **334**, 113320**.**
7. A.F. Carvalho, A.J.S. Fernandes, C. Leitão, J. Deuermeier, A.C. Marques, R. Martins, E. Fortunato and F.M. Costa, Laser-induced graphene strain sensors produced by ultraviolet irradiation of polyimide, *Adv. Funct. Mater.*, 2018, **28**(52), 1805271.
8. S.Y. Jeong, Y.W. Ma, J.U. Lee, G.J. Je and B.S. Shin, Flexible and highly sensitive strain sensor based on laser-induced graphene pattern fabricated by 355 nm pulsed laser, *Sensors (Basel)*, 2019, **19**(22), 4867.
9. T. Han, A. Nag, R.B.V.B. Simorangkir, N. Afsarimanesh, H.R. Liu, S.C. Mukhopadhyay, Y.Z. Xu, M. Zhadobov and R. Sauleau, Multifunctional flexible sensor based on laser-induced graphene, *Sensors*, 2019, **19**, 3477.
10. D.Y. Wang, L.Q. Tao, Y. Liu, T.Y. Zhang, Y. Pang, Q. Wang, S. Jiang, Y. Yang and T.L. Ren, High performance flexible strain sensor based on self-locked overlapping graphene sheets, *Nanoscale*, 2016, **8**(48), 20090-20095.
11. X.W. Fu, Z.M. Liao, J.X. Zhou, Y.B. Zhou, H.C. Wu, R. Zhang, G.Y. Jing, J. Xu, X.S. Wu, W.L. Guo and D.P. Yu, Strain dependent resistance in chemical vapor deposition grown graphene, *Appl. Phys. Lett.*, 2011, **99**(21), 213107.
12. X. Li, R.J. Zhang, W.J. Yu, K.L. Wang, J.Q. Wei, D.H. Wu, A.Y. Cao, Z.H. Li, Y. Cheng, Q.S. Zheng, R.S. Ruoff and H.W. Zhu, Stretchable and highly sensitive graphene-on-polymer strain sensors, *Sci. Rep.*, 2012, **2**, 870.
13. Q.M. Li, H. Liu, S.D. Zhang, D.B. Zhang, X.H. Liu, Y.X. He, L.W. Mi, J.X. Zhang, C.T. Liu, C.Y. Shen and Z.H. Guo, Superhydrophobic electrically conductive paper for ultrasensitive strain sensor with excellent anticorrosion and self-cleaning property, *ACS Appl. Mater. Interfaces*, 2019, **11**(24), 21904-21914.
14. J. Lee, S. Pyo, D.S. Kwon, E. Jo, W. Kim and J. Kim, Ultrasensitive strain sensor based on separation of overlapped carbon nanotubes, *Small*, 2019, **15**(12), 21904-21914.
15. T. Yamada, Y. Hayamizu, Y. Yamamoto, Y. Yomogida, A. Izadi-Najafabadi, D.N. Futaba and K. Hata, A stretchable carbon nanotube strain sensor for human-motion detection, *Nat. Nanotechnol.*, 2011, **6**(5), 296-301.
16. M. Amjadi, A. Pichitpajongkit, S. Lee, S. Ryu and I. Park, Highly stretchable and sensitive strain sensor based on silver nanowire-elastomer nanocomposite, *ACS Nano*, 2014, **8**(5), 5154-5163.

17. N. Tang, C. Zhou, D.Y. Qu, Y. Fang, Y.B. Zheng, W.W. Hu, K. Jin, W.W. Wu, X.X. Duan and H. Haick, A highly aligned nanowire-based strain sensor for ultrasensitive monitoring of subtle human motion, *Small*, 2020, **16**(24), 2001363.